

# We are IntechOpen, the world's leading publisher of Open Access books Built by scientists, for scientists

**4,800**

Open access books available

**122,000**

International authors and editors

**135M**

Downloads

Our authors are among the

**154**

Countries delivered to

**TOP 1%**

most cited scientists

**12.2%**

Contributors from top 500 universities



**WEB OF SCIENCE™**

Selection of our books indexed in the Book Citation Index  
in Web of Science™ Core Collection (BKCI)

Interested in publishing with us?  
Contact [book.department@intechopen.com](mailto:book.department@intechopen.com)

Numbers displayed above are based on latest data collected.  
For more information visit [www.intechopen.com](http://www.intechopen.com)



# Fault-Tolerant Attitude Estimation for Satellite using Federated Unscented Kalman Filter

Jonghee Bae, Seungho Yoon, and Youdan Kim

*School of Mechanical and Aerospace Engineering, Seoul National University,  
Republic of Korea*

## 1. Introduction

Satellites provide various services essential to the modern life of human being. For example, satellite images are used for many applications such as reconnaissance, geographic information system, etc. Therefore, design and operation requirements of the satellite system have become more severe, and also the system reliability during the operation is required. Satellite attitude control systems including sensors and actuators are critical subsystems, and any fault in the satellite control system can result in serious problems. To deal with this problem, various attitude estimation algorithms using multiple sensors have been actively studied for fault tolerant satellite system (Edelmayer & Miranda, 2007; Jiancheng & Ali, 2005; Karlgaard & Schaub, 2008; Kerr, 1987; Xu, 2009).

Satellites use various attitude sensors such as gyroscopes, sun sensors, star sensors, magnetometers, and so on. With these sensors, satellite attitude information can be obtained using the estimation algorithms including Kalman filter, extended Kalman filter (EKF), unscented Kalman filter (UKF), and particle filter. Agrawal et al. and Nagendra et al. presented the attitude estimation algorithm based on Kalman filter for satellite system (Agrawal & Palermo, 2002; Nagendra et al., 2002). Mehra and Bayard dealt with the problems of satellite attitude estimation based on the EKF algorithm using the gyroscope and star tracker as attitude sensors (Mehra & Bayard, 1995). In the EKF algorithm, the nonlinearities of the satellite system are approximated by the first-order Taylor series expansion, and therefore it sometimes provides undesired estimates when the system has severe nonlinearities. Recently, researches on UKF have been performed because the UKF can capture the posterior mean and covariance to the third order of nonlinear system. It is known that the UKF can provide better results for the estimation of highly nonlinear systems than EKF (Crassidis & Markley, 2003; Jin et al., 2008; Julier & Uhlmann, 2004). Crassidis and Markley proposed the attitude estimation algorithm based on unscented filter, and showed that the fast convergence can be obtained even with inaccurate initial conditions. The UKF was used to solve the relative attitude estimation problem using the modified Rodriguez parameter (MRP), where the gyroscope, star tracker, and laser rendezvous radar were employed as the attitude sensors (Jin et al., 2008).

For multi-sensor systems, there are two different filter schemes for the measured sensor data process: centralized Kalman filter (CKF) and decentralized Kalman filter (DKF) (Kim & Hong, 2003). In the CKF, all measured sensor data are processed in the center site, and

therefore information loss can be minimized. However, it causes severe computational problem and may provide unreliable results, when the CKF is overloaded with more data than it can handle. In the DKF, the local estimators of each sensor can generate the global optimal or suboptimal state estimates according to the data fusion criterion. Wei and Schwarz presented a decentralized Kalman filter strategy and applied to GSP/INS integration (Wei & Schwarz, 1990). Edelmayer and Miranda applied the decentralized extended Kalman filter to the fault tolerant estimation (Edelmayer & Miranda, 2007). A decentralized unscented Kalman filter in federated configuration was developed for multi-sensor navigation data fusion (Jiancheng & Ali, 2005). Jiancheng and Ali used the inertial navigation system (INS) integrated with astronavigation system and global positioning system (GPS). In (Kim & Hong, 2003; Lee, 2008), a decentralized information filter was proposed by combining unscented transformation method with the extended information filtering architecture, and the algorithm was extended to perform the decentralized estimation for sensor networks. The decentralized scheme has advantages in the sense that (i) much more data can be treated because of the parallel structure, and (ii) the fault can be easily detected and isolated due to the decentralized scheme (Bae & Kim, 2010; Edelmayer & Miranda, 2007).

In this study, the decentralized Kalman filter scheme in a federated configuration is adopted for satellite attitude estimation. The federated UKF can be employed to detect and isolate the sensor fault effectively (Jiancheng & Ali, 2005; Edelmayer & Miranda, 2007). Using the fault detection and isolation (FDI) algorithm, the accurate attitude information can be provided despite sensor fault occurrence, and therefore satellite can perform its mission continuously. There exist various FDI algorithms (Hwang et al., 2010). Fault can be detected and identified by (i) monitoring the measurement residual, or (ii) using sensitivity factor. In this study, sensitivity factor is used to detect and identify the sensor failure. To verify the performance of the proposed algorithm, numerical simulations are performed for a satellite with gyroscope and star tracker as attitude sensor. The numerical simulation shows that the federated UKF with FDI algorithm detects and isolates the sensor faults effectively, and therefore it provides accurate and robust attitude estimation results when the attitude sensor has a fault.

This paper is organized as follows. In Section 2, the attitude kinematics, dynamics, and sensor modeling are described. The attitude estimation algorithms using UKF and the federated configuration, and FDI algorithm are derived in Section 3. Numerical simulation and analysis to verify the proposed algorithm are shown in Section 4. Finally, conclusions are presented in Section 5.

## 2. Attitude kinematics, dynamics, and sensor modeling

### 2.1 Attitude kinematics and dynamics

In this study, quaternion is used for describing attitude dynamics of satellite (Schaub & Junkins, 2003). The quaternion is a four-dimensional vector, defined as

$$q = [q_1 \quad q_2 \quad q_3 \quad q_4]^T \equiv [\hat{q} \quad q_4]^T \quad (1)$$

where

$$\hat{q} = [q_1 \quad q_2 \quad q_3]^T = \hat{e} \sin\left(\frac{\mathcal{S}}{2}\right) \tag{2}$$

$$q_4 = \cos\left(\frac{\mathcal{S}}{2}\right) \tag{3}$$

where  $\hat{e}$  is the unit Euler axis, and  $\mathcal{S}$  is the rotation angle. The quaternion satisfies the following constraint.

$$q^T q = q_1^2 + q_2^2 + q_3^2 + q_4^2 = 1 \tag{4}$$

The direction cosine matrix can be written in terms of quaternion as

$$A(q) = (q_4^2 - \|\hat{q}\|^2) I_{3 \times 3} + 2\hat{q}\hat{q}^T - 2q_4\hat{q}^\times = \Xi^T(q)\Psi(q) \tag{5}$$

where  $I_{3 \times 3}$  is a  $3 \times 3$  identity matrix and

$$\Xi(q) = \begin{bmatrix} q_4 I_{3 \times 3} + \hat{q}^\times \\ -\hat{q}^T \end{bmatrix} \tag{6}$$

$$\Psi(q) = \begin{bmatrix} q_4 I_{3 \times 3} - \hat{q}^\times \\ -\hat{q}^T \end{bmatrix} \tag{7}$$

Also,  $\hat{q}^\times$  is the cross-product matrix defined by

$$\hat{q}^\times = \begin{bmatrix} 0 & -q_3 & q_2 \\ q_3 & 0 & -q_1 \\ -q_2 & q_1 & 0 \end{bmatrix} \tag{8}$$

The kinematic differential equation for the quaternion is given by

$$\dot{q} = \frac{1}{2} \Xi(q) \omega = \frac{1}{2} \Omega(\omega) q \tag{9}$$

where  $\omega$  is the three-dimensional angular rate vector and

$$\Omega(\omega) = \begin{bmatrix} -\omega^\times & \omega \\ -\omega^T & 0 \end{bmatrix} \tag{10}$$

Quaternion provides successive rotation using quaternion multiplication as

$$A(q(t_1))A(q(t_2)) = A(q(t_1) \otimes q(t_2)) \tag{11}$$

The composition of the quaternion is defined by

$$q(t_1) \otimes q(t_2) = [\Psi(q(t_1)) \quad q(t_1)] q(t_2) = [\Xi(q(t_2)) \quad q(t_2)] q(t_1) \tag{12}$$

Also, the inverse quaternion is defined by

$$q^{-1} = \begin{bmatrix} -\hat{q} \\ q_4 \end{bmatrix} \quad (13)$$

Note that  $q \otimes q^{-1} = [0 \ 0 \ 0 \ 1]^T$ , which is the identity quaternion.

The attitude dynamics of a spacecraft can be represented from the Euler's momentum equation as follows (Schaub & Junkins, 2003).

$$J\dot{\omega} = -\omega^\times J\omega + \tau \quad (14)$$

where  $J$  is a  $3 \times 3$  moment of inertia matrix, and  $\tau \in R^3$  is a control torque vector.

## 2.2 Sensor modeling

### 2.2.1 Gyroscope model

A gyroscope is a general sensor that measures the angular rate of the satellite. The gyroscope system can be expressed mathematically by Frarrenkopf's model (Karlgaard & Schaub, 2008). In this model, the measured angular velocity is represented by the sum of the true angular velocity, an additive bias, and Gaussian white-noise. The bias dynamics are considered to be driven by a Gaussian white-noise process. Also, in this model, it is assumed that the bias term can be regarded as the net effect of several systematic error sources such as scale factor errors, non-orthogonality, misalignment, and so on. The gyroscope model can be represented as

$$\tilde{\omega} = \omega + \beta + \eta_v \quad (15)$$

$$\dot{\beta} = \eta_u \quad (16)$$

where  $\tilde{\omega}$  is the measured angular velocity,  $\omega$  is the true angular velocity,  $\beta$  is the drift, and  $\eta_v$  and  $\eta_u$  are independent zero-mean Gaussian white-noise processes with

$$E[\eta_v(t)\eta_v^T(\tau)] = \sigma_v^2 \delta(t-\tau) I_{3 \times 3} \quad (17)$$

$$E[\eta_u(t)\eta_u^T(\tau)] = \sigma_u^2 \delta(t-\tau) I_{3 \times 3} \quad (18)$$

where  $E[\ ]$  denotes expectation, and  $\delta(t-\tau)$  is the Dirac-delta function.

### 2.2.2 Star tracker model

The rate signal from the gyroscope is integrated to estimate the attitude of the satellite, and therefore it causes a drift of the estimates away from the true value. For this reason, it is necessary to use additional sensors such as a star tracker for the compensation of the drift error. A star tracker is an optimal device, which recognizes the star pattern and provides the attitude information of a spacecraft (Jayaraman et al., 2006). The output of the star tracker is an estimated quaternion that relates the orientation of the body with respect to the inertial

frame. The quaternion estimates are assumed to be unbiased, but it contains a random measurement noise. A star tracker model can be represented as (Karlgaard & Schaub, 2008)

$$q_s = \delta q_s \otimes q \quad (19)$$

where  $q_s$  is a star tracker output vector which is a continuously measured quaternion vector,  $q$  is the quaternion representing the true orientation, and  $\delta q_s$  is an independent zero-mean Gaussian white-noise process with

$$E[\delta q_s(t)] = 0 \quad (20)$$

$$E[\delta q_s(t)\delta q_s^T(\tau)] = \sigma_s^2 \delta(t - \tau) I_{4 \times 4}. \quad (21)$$

### 3. Fault-tolerant attitude estimation

To incorporate the various sensor data of the multi-sensor system, there are two schemes which provide accurate and robust state estimation: CKF and DKF. The decentralized scheme in a federated configuration has the benefit of detecting a fault in a local sensor during the process. Therefore, a federated UKF is adopted to detect and isolate the sensor faults, in this study. Federated UKF algorithm can prevent mission failures because an effective FDI algorithm is employed in the federated configuration.

#### 3.1 Federated configuration filter

Federated filtering consists of two parts: local filters and master filter. The local filters are parallel processed and independent of each other, and the estimated results of the local filters are fused in the master filter. In each local filter, local estimate is obtained using the measurements of the local sensors. The master filter uses the estimates of the local filters to update the global state estimate in a fusion process, and this result is used for the initialization of the local filters. Federated filtering scheme has an advantage; it can detect and isolate the fault of the local sensor during the process. The master filter is not affected by the failure of the local sensor (Edelmayer & Miranda, 2007; Jiancheng & Ali, 2005). The structure of the federated configuration filter is shown in Fig. 1. The filtering algorithm based on UKF in the local filter and the data fusion in the master filter are explained in the subsequent sections, respectively.

#### 3.2 Local filter: unscented Kalman filter

For the satellite attitude estimation, several algorithms have been studied: Kalman filter, EKF, UKF, and particle filter. The EKF is widely used for the state estimation of the nonlinear systems. The EKF is based on approximating the nonlinearities by the first-order Taylor series expansion, and therefore this filter may sometimes provide unreliable estimates if the system has severe nonlinearities. On the other hand, the UKF is the extension of the Kalman filter to reduce the linearization errors of the EKF. It is known that the UKF provides good estimation results not only for linear systems but also for nonlinear systems. In this study, the UKF is considered to estimate the attitude of the satellite.

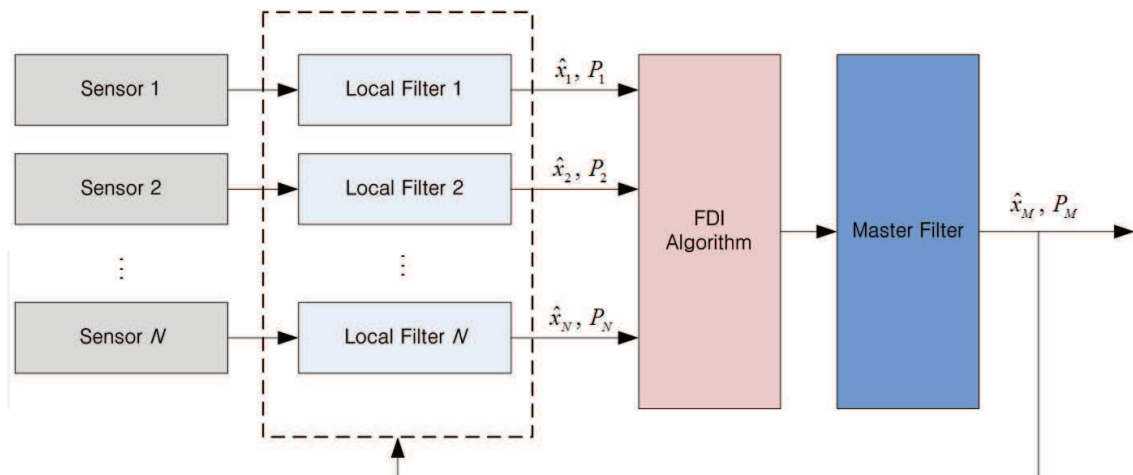


Fig. 1. The structure of the federated filter

Consider the  $n$ -state nonlinear system for UKF algorithm (Simon, 2006).

$$\begin{aligned} x_{k+1} &= f(x_k, u_k, t_k) + w_k, & w_k &\sim N(0, Q_k) \\ z_k &= h(x_k, t_k) + v_k, & v_k &\sim N(0, R_k) \end{aligned} \quad (22)$$

where  $x_k \in \mathfrak{R}^n$  is the state vector,  $z_k \in \mathfrak{R}^m$  is the measurement vector,  $w_k \in \mathfrak{R}^n$  is the process noise vector, and  $v_k \in \mathfrak{R}^m$  is the measurement noise vector. It is assumed that the noise vectors are uncorrelated white Gaussian process. The UKF is initialized as follows.

$$\begin{aligned} \hat{x}_0^+ &= E[x_0] \\ P_0^+ &= E\left[(x_0 - \hat{x}_0^+)(x_0 - \hat{x}_0^+)^T\right] \end{aligned} \quad (23)$$

The UKF is derived based on the unscented transformation which is simpler to approximate a Gaussian distribution than to approximate an arbitrary nonlinear function. A set of sigma points is first chosen which are selected to express the probability distribution, and the mean and covariance of the set of sigma points are  $\bar{x}$  and  $P$ . The nonlinear function is then applied to each sigma point, and the results provide a set of transformed points with the mean and covariance. Now, time update is performed to propagate the state estimate and covariance from one measurement time to the next. To propagate from time step  $(k-1)$  to  $k$ , the set of sigma points is chosen using the current best guess of the mean and covariance as follows.

$$\begin{aligned} \hat{x}_{k-1}^i &= \hat{x}_{k-1}^+ + \tilde{x}^i \\ \tilde{x}^i &= \left(\sqrt{nP_{k-1}^+}\right)_i^T & i &= 1, \dots, n \\ \tilde{x}^{n+i} &= -\left(\sqrt{nP_{k-1}^+}\right)_i^T & i &= 1, \dots, n \end{aligned} \quad (24)$$

For the state propagation, *a priori* state estimate  $\hat{x}_k^-$  and error covariance  $P_k^-$  are computed using the propagated sigma point vectors as

$$\hat{x}_k^i = f(\hat{x}_{k-1}^i, u_k, t_k) \tag{25}$$

$$\hat{x}_k^- = \frac{1}{2n} \sum_{i=1}^{2n} \hat{x}_k^i \tag{26}$$

$$P_k^- = \frac{1}{2n} \sum_{i=1}^{2n} (\hat{x}_k^i - \hat{x}_k^-)(\hat{x}_k^i - \hat{x}_k^-)^T + Q_{k-1} \tag{27}$$

where  $\hat{x}_k^i$  denotes the transformed sigma points using the nonlinear function. Then, the measurement update is performed using the time propagation results. Sigma points are again chosen with the appropriate changes using the current best guess of the mean and covariance.

$$\begin{aligned} \hat{x}_k^i &= \hat{x}_k^- + \tilde{x}^i \\ \tilde{x}^i &= \left(\sqrt{nP_k^-}\right)_i^T & i = 1, \dots, n \\ \tilde{x}^{n+i} &= -\left(\sqrt{nP_k^-}\right)_i^T & i = 1, \dots, n \end{aligned} \tag{28}$$

Each predicted measurement vector  $\hat{z}_k^i$  is obtained through the measurement model, and the predicted measurement  $\hat{z}_k$  is calculated as follows.

$$\hat{z}_k^i = h(\hat{x}_k^i, t_k) \tag{29}$$

$$\hat{z}_k = \frac{1}{2n} \sum_{i=1}^{2n} \hat{z}_k^i \tag{30}$$

The innovation covariance  $P_{zz}$  and the cross correlation  $P_{xz}$  are obtained with the assumption that the measurement noise is additive and independent as follows.

$$P_{zz} = \frac{1}{2n} \sum_{i=1}^{2n} (\hat{z}_k^i - \hat{z}_k)(\hat{z}_k^i - \hat{z}_k)^T + R_k \tag{31}$$

$$P_{xz} = \frac{1}{2n} \sum_{i=1}^{2n} (\hat{x}_k^i - \hat{x}_k^-)(\hat{z}_k^i - \hat{z}_k)^T \tag{32}$$

Finally, *a posteriori* state and covariance estimates can be performed using the predicted values as

$$\hat{x}_k^+ = \hat{x}_k^- + K_k(z_k - \hat{z}_k) \tag{33}$$

$$P_k^+ = P_k^- - K_k P_{zz} K_k^T \tag{34}$$

where  $K_k$  is the filter gain selected to minimize the mean squared error of the estimate as



$$K_k = P_{xz} P_{zz}^{-1} \quad (35)$$

This completes the UKF algorithms. Note that the EKF algorithm is based on the linearization while the UKF algorithm is based on the unscented transformations which are more accurate than the linearization for propagating mean and covariance.

### 3.3 Master filter: data fusion

The master filter is processed at the same rate of the local filter. If all local estimates are uncorrelated, the global estimate from the master filter is given by

$$\hat{x}_M = P_M \{ P_1^{-1} \hat{x}_1 + P_2^{-1} \hat{x}_2 + \dots + P_N^{-1} \hat{x}_N \} \quad (36)$$

$$P_M^{-1} = P_1^{-1} + P_2^{-1} + \dots + P_N^{-1} \quad (37)$$

where  $\hat{x}_i$  and  $P_i$  are the local estimate and its covariance of the  $i$ -th local filter, and  $P_M^{-1}$  is called the information matrix. Note that the global estimate is the sum of local estimates and linear weighted combination with weighting matrices,  $P_i^{-1}$  ( $i = 1, 2, \dots, N$ ), and  $P_M^{-1}$ .

The federated UKF scheme has two operating modes according to initializing the local filter of the fused data: reset mode and no-reset mode. In the reset mode, the local filters are initiated by the global estimate as follows:

$$\begin{aligned} \hat{x}_i &= \hat{x}_M \\ P_i &= \beta_i^{-1} P_M \end{aligned} \quad (38)$$

where  $\beta_i$  is the information sharing coefficient satisfying  $\beta_1 + \beta_2 + \dots + \beta_N + \beta_M = 1$ . This mode provides a continuous information feedback from the master filter to the local filters. In the no-reset mode, on the other hand, information is not feedback, and thereby the global fused data does not have an effect on the local filters. Also, local filters retain their information which is given locally. It is known that the reset mode can provide accurate estimates, while the no-reset mode gives the tolerance of sensor failure. In this study, the reset mode in the federated configuration filter is used to obtain better and more accurate estimation values. Instead, the FDI algorithm is adopted for the fault tolerance as described in the next subsection.

### 3.4 Fault detection and isolation algorithm

The federated UKF provides accurate and robust state estimation values, when all attitude sensors normally operate during the maneuver. However, if one of the attitude sensors has a problem, the performance of the federated UKF is degraded. To overcome this problem, the FDI algorithm is employed in the federated configuration.

Fault detection usually requires the careful monitoring of the measured output data. In normal situation, the output data follow the known patterns of evolution under the condition of the limited random disturbance and measurement noise. However, the measured output data change their nominal evolution pattern, when sensor failures occur. Fault detection algorithms are generally based on considering the differences between the evolution patterns and the measured output data (Bae & Kim, 2010).

General fault detection algorithms are monitoring the measurement residual and utilizing the sensitivity factor. In this study, the sensitivity factor is used to detect the sensor failure. The sensitivity factor is defined as follows.

$$S_i = (\hat{x}_i - \hat{x}_M)^T (P_i + P_M)^{-1} (\hat{x}_i - \hat{x}_M) \tag{39}$$

When  $S_i$  is smaller than a threshold value, then  $i$ -th sensor is considered as a healthy one, and therefore the sensor output can be used to calculate the global estimates  $\hat{x}_M$  and  $P_M$ . However, if  $S_i$  is larger than a threshold value, then  $i$ -th sensor might have some problems. In this case, the global estimates  $\hat{x}_M$  and  $P_M$  should be computed without using the output of  $i$ -th sensor, that is a faulty one. The threshold value can be selected based on Chi-square distribution and optimized by the experiment for the particular application. Figure 2 shows the time histories of the sensitivity factor for the sensor normal case and the sensor failure case.

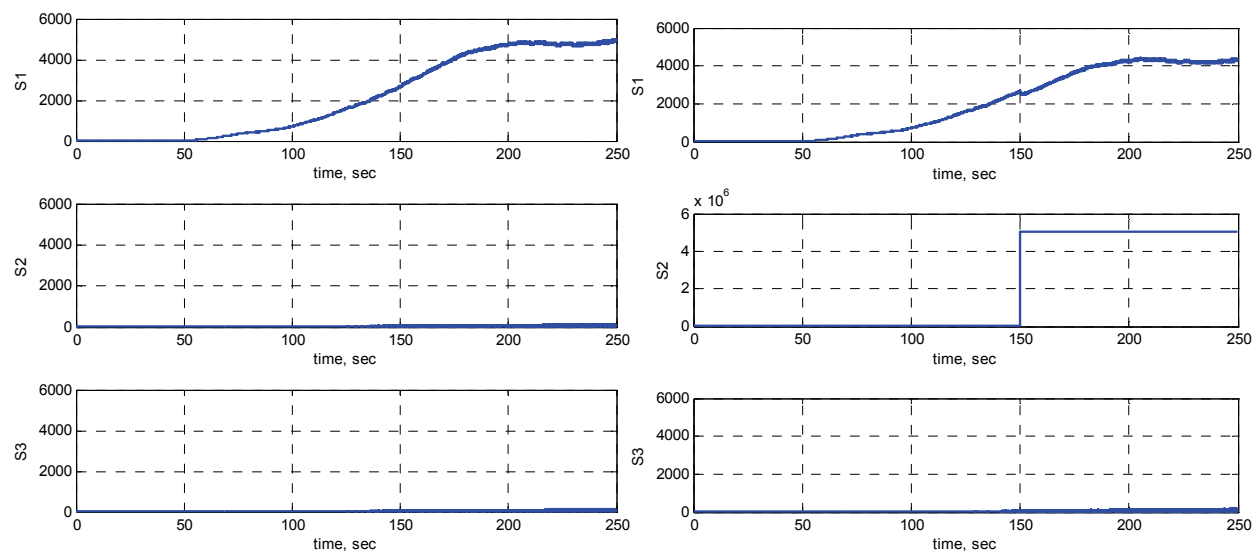


Fig. 2. Time histories of sensitivity factor: (a) normal case (left), (b) failure case (right)

Figure 2 (a) illustrates the sensitivity factor histories for normal sensors. The sensitivity factor of the first sensor is larger than others. This is because less accuracy of the first sensor leads to provide less reliable state estimate and covariance. Therefore the corresponding first sensitivity factor is large compared with others. Figure 2 (b) shows the sensitivity factor histories when the fault of the second sensor occurs at 150 seconds. This failure causes a significantly large sensitivity factor after 150 seconds compared with Fig. 2 (a). The change of the sensitivity factor is larger than the threshold value, and the fault of the second sensor can be detected and isolated.

#### 4. Numerical simulation and analysis

Numerical simulations are performed to verify the performance of the proposed attitude estimation algorithm based on the federated UKF. In the simulation, two types of attitude sensors are considered to estimate the attitude of the satellite: one gyroscope and two star trackers. The integrated system of the gyroscope and the star tracker provides accurate

estimates in spite of the sensor uncertainties such as drift, scale factor errors, shutting off the power, etc.

Two failure cases in each attitude sensor are considered: (i) the fault in the gyroscope, and (ii) the fault in the star tracker. The fault detection index is defined as summarized in Table 1. Note that the fault detection index is 0 when all sensors are normal. The fault detection index 1 indicates the fault of the gyroscope, the index 2 indicates the fault of the star tracker A, and the index 3 indicates the fault of the star tracker B, respectively.

Sensor fault type	Fault detection index
No sensor fault	0
Gyroscope fault	1
Star tracker A fault	2
Star tracker B fault	3

Table 1. Fault detection index

The quaternion history in a normal condition is considered as a reference. Sensor fault is not included in the normal condition. The time histories of the reference quaternion are shown in Fig. 3. Initial quaternion of all simulations is chosen as

$$q(t_0) = [0 \ 0 \ 0 \ 1]^T.$$

The local estimates and the global estimate are shown in Fig. 4. The quaternion estimates in the local and master filters are perfectly matched to the true values shown in Fig. 3, because all sensors are healthy. The attitude errors between true quaternion and the estimated quaternion are shown in Fig. 5. The first three windows from the top present the estimated attitude in three local filters, and the last window presents the global estimate in the master filter. The magnitude of the error is less than 0.05 between true quaternion and the estimated quaternion in the gyroscope. The magnitude of the error in the star tracker A and B is less than 0.02. In the master filter, the magnitude of the error between true quaternion and the global estimate is less than 0.02 since three sensor signals are fused as described in Eqs. (36)-(38).

#### 4.1 Failure in the gyroscope

In this section, a sudden failure in the gyroscope is considered to verify the fault-tolerant performance. A failure of the gyroscope occurs at 100 seconds, and the output signals from the gyroscope to the corresponding local filter are zero after 100 seconds. The time histories of quaternion measured by the gyroscope, the star tracker A, and the star tracker B are shown in Fig. 6. The estimation results without the FDI algorithm are shown in Figs. 7 and 8. The local and global estimates are shown in Fig. 7, and the attitude errors between true quaternion and the estimated quaternion are shown in Fig. 8. The estimation results with the FDI algorithm are shown in Figs. 9 and 10. The local and global estimates are shown in Fig. 9, and the attitude errors are shown in Fig. 10. Fault detection and isolation result is presented in Fig. 11 with the fault detection index defined in Table 1.

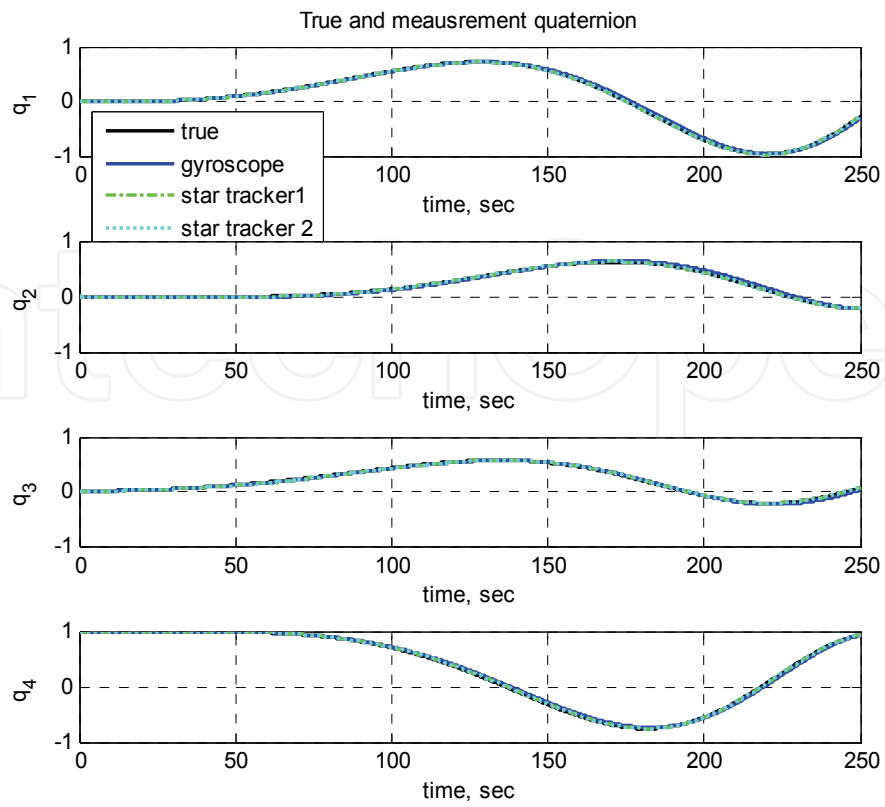


Fig. 3. Quaternion history (normal condition)

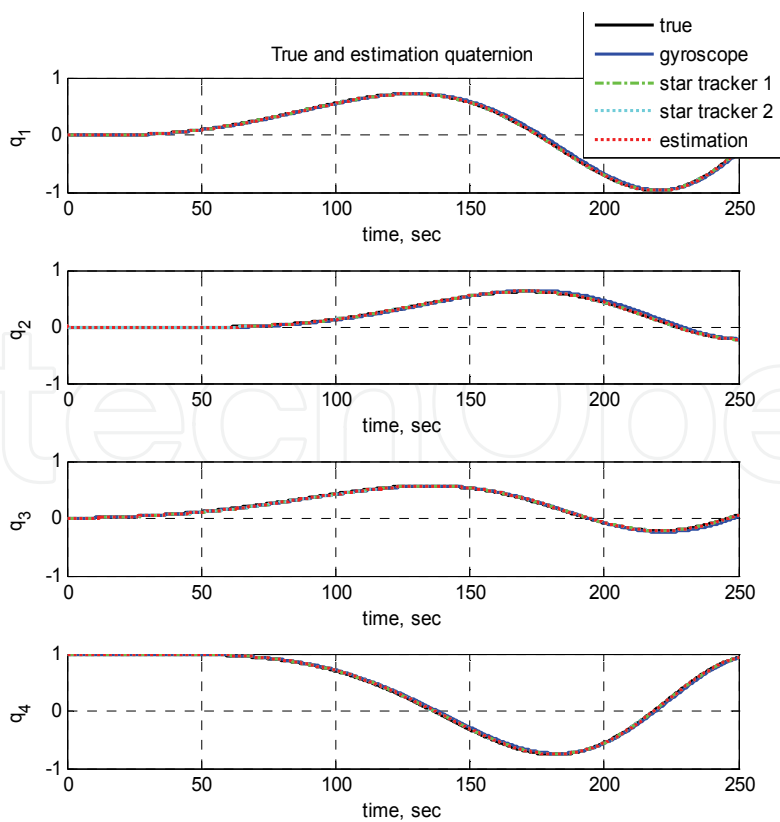


Fig. 4. Local and global estimates (normal condition)

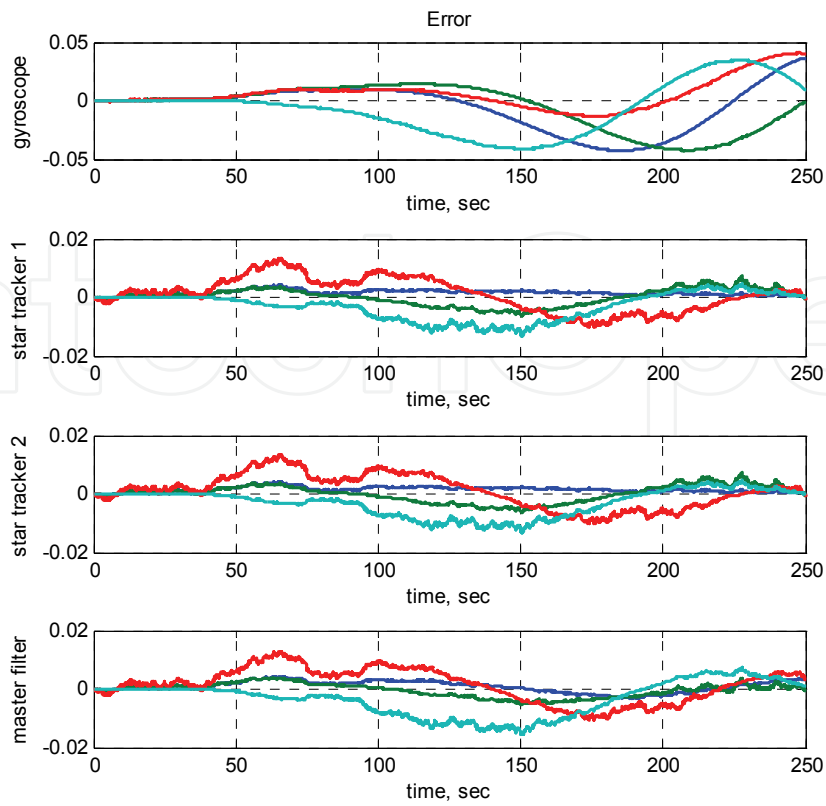


Fig. 5. Error between true quaternion and estimates (normal condition)

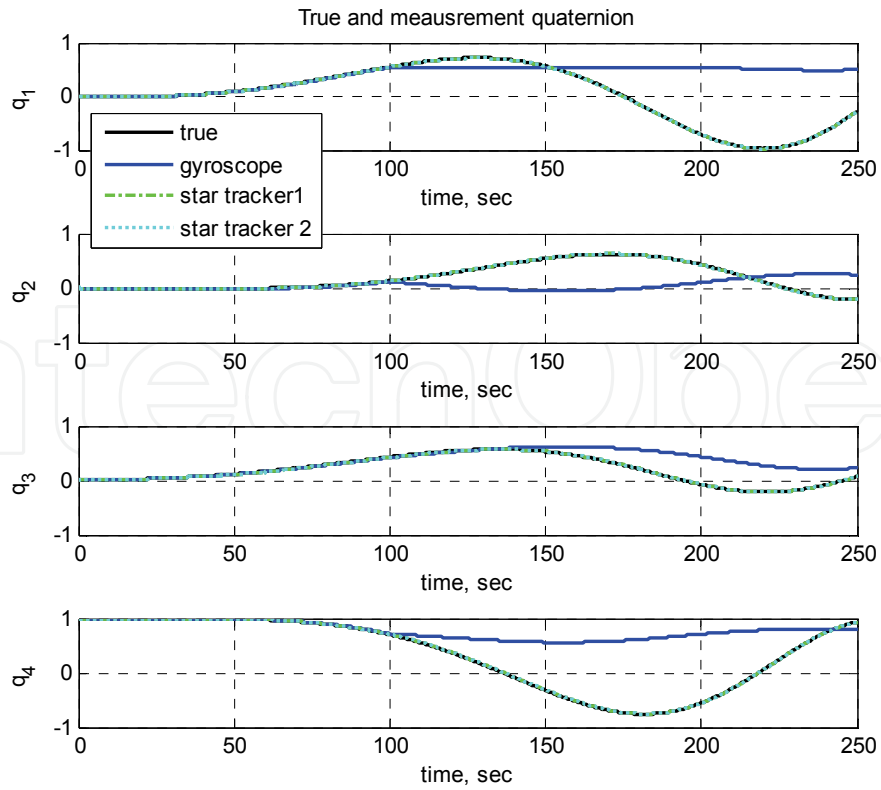


Fig. 6. Quaternion history (gyroscope fault)

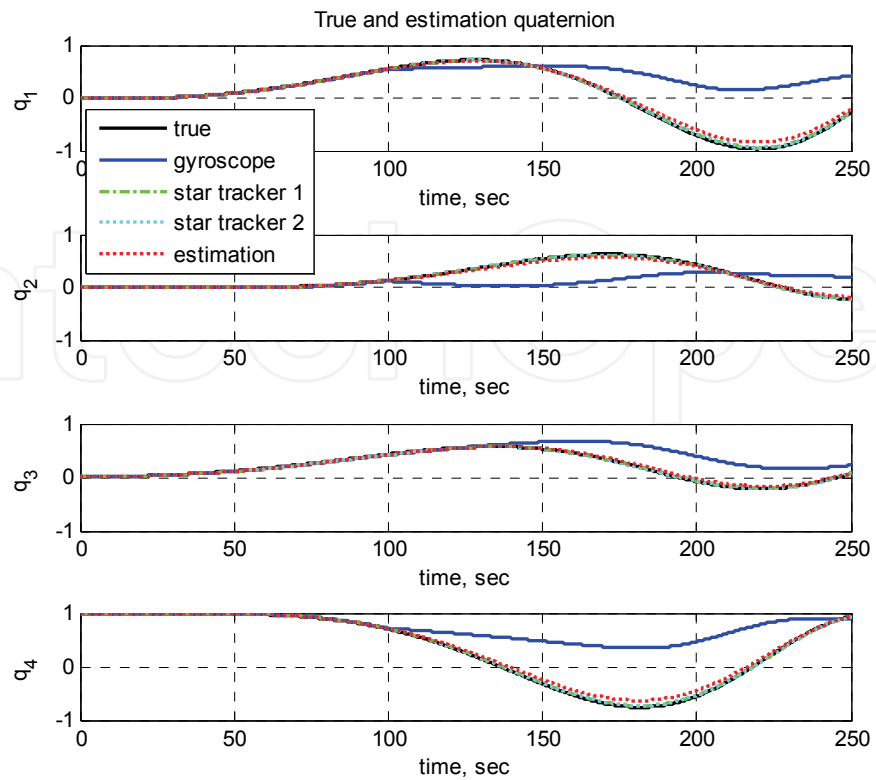


Fig. 7. Local and global estimates without FDI algorithm (gyroscope fault)

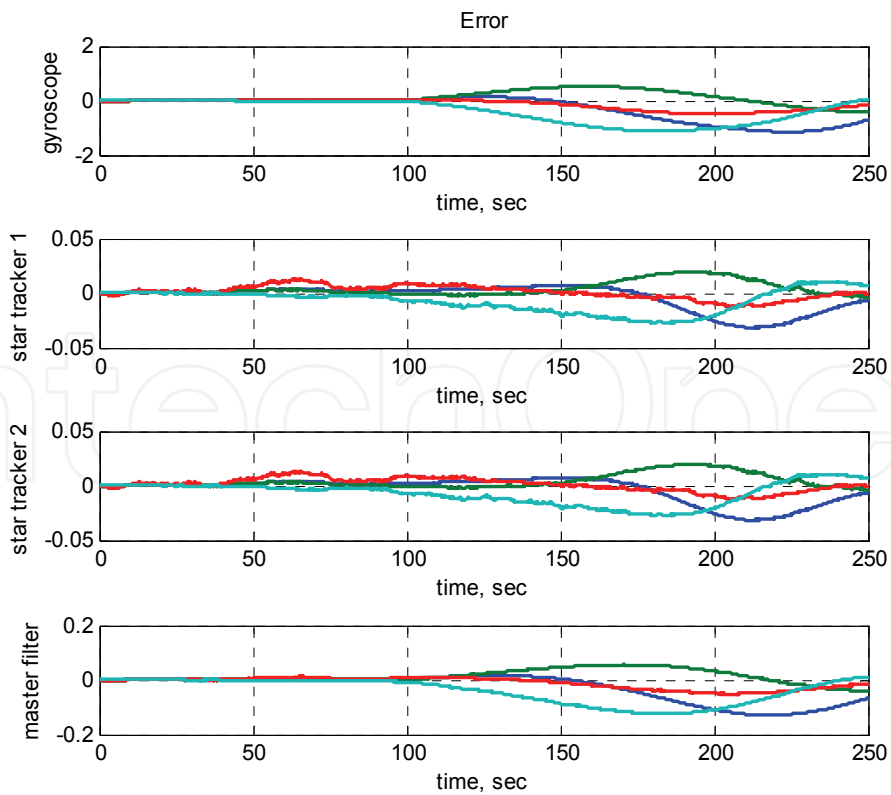


Fig. 8. Error between true quaternion and estimates without FDI algorithm (gyroscope fault)

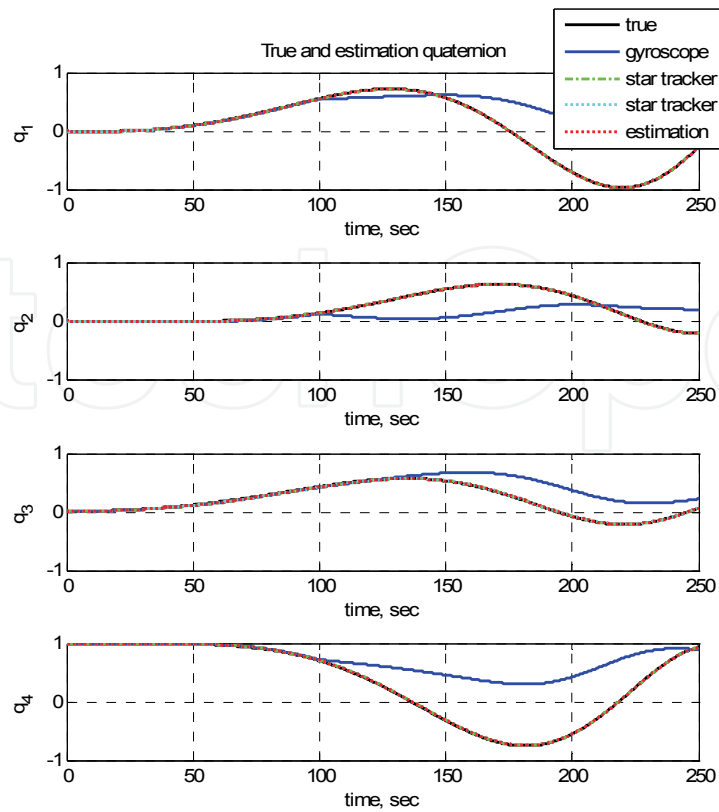


Fig. 9. Local and global estimates with FDI algorithm (gyroscope fault)

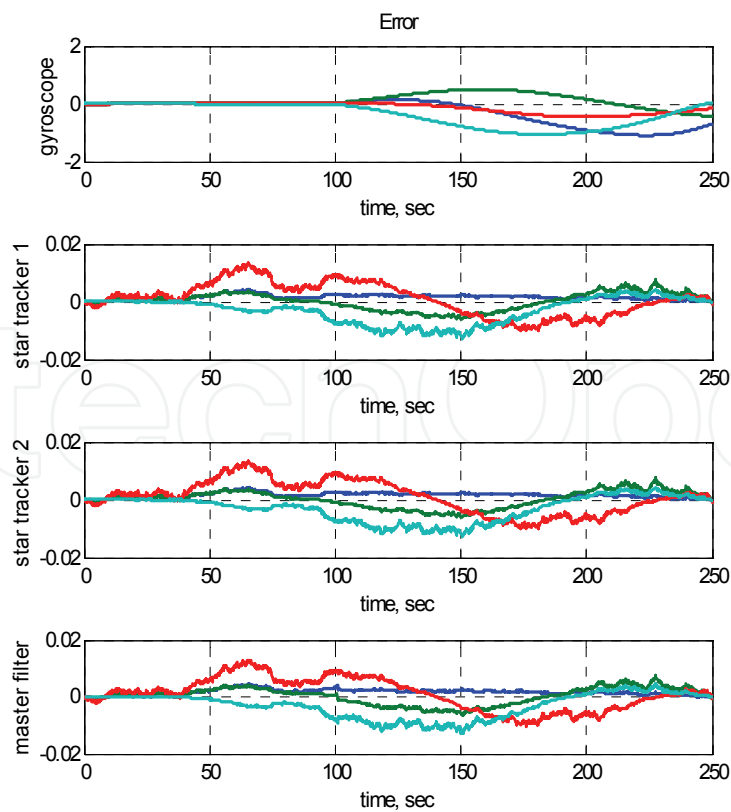


Fig. 10. Error between true quaternion and estimates with FDI algorithm (gyroscope fault)

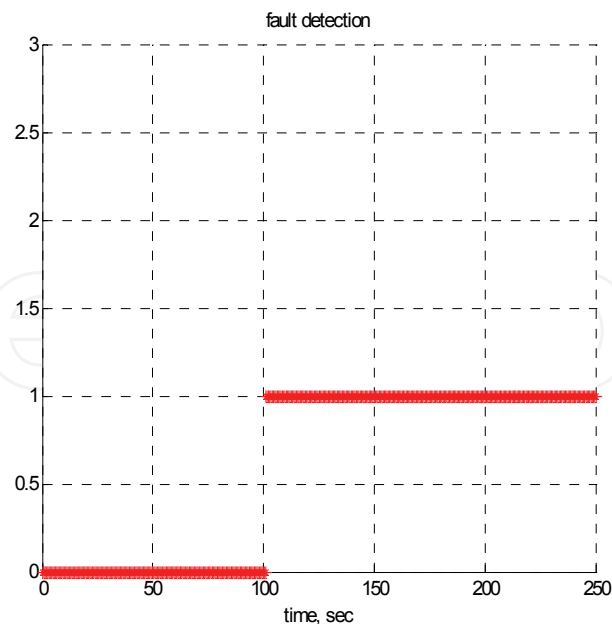


Fig. 11. Fault detection index (gyroscope fault)

As shown in Fig. 8, the maximum magnitude of the error between true quaternion and the local estimate in the gyroscope increases from 0.05 to 1.21 due to the sudden fault in the gyroscope at 100 seconds. At the same time, the maximum magnitude of the error in the master filter increases from 0.02 to 0.2. This error increase in the master filter is because the global estimate is calculated using not only healthy sensors but also the faulty sensor. Although the fault detection and isolation is not performed, the magnitude of the global estimate in the master filter is less than 0.2 as shown in Fig. 8. This result comes from the federated configuration. As shown in Fig. 10, the magnitude of the global estimate in the master filter becomes less than 0.02 when the fault detection and isolation is applied. Note that, when all sensors are normal, the maximum magnitude of the error in the gyroscope is less than 0.05 and the maximum magnitude of the error in the master filter is less than 0.02 as illustrated in Fig. 5. Consequently, the federated UKF reduces the attitude error from 1.21 (in the gyroscope) to 0.2 (in the master filter), and the FDI algorithm in the federated configuration reduces the attitude error of the master filter from 0.2 to 0.02.

#### 4.2 Failure in the star tracker A

In this section, a sudden failure in the star tracker A is considered to verify the fault-tolerant performance. A failure of the star tracker A occurs at 100 seconds, and the output signals from the star tracker A are zero after 100 seconds. The time histories of quaternion measured by the gyroscope, the star tracker A, and the star tracker B are shown in Fig. 12. The estimation results without the FDI algorithm are shown in Figs. 13 and 14. The local and global estimates are shown in Fig. 13, and the attitude errors between true quaternion and the estimated quaternion are shown in Fig. 14. The estimation results with the FDI algorithm are shown in Figs. 15 and 16. The local and global estimates are shown in Fig. 15, and the attitude errors are shown in Fig. 16. Fault detection and isolation result is presented in Fig. 17 with the fault detection index defined in Table 1.

As shown in Fig. 14, the maximum magnitude of the error between true quaternion and the local estimates in all sensors is suddenly increased due to the sudden fault in the star tracker



A at 100 seconds: the errors in the gyroscope and the star tracker B exceed 0.1, and the error in the star tracker A exceeds 0.8. The maximum magnitude of the error in the master filter increases from 0.02 to 0.48. Similar to the gyroscope fault case described in Section 4.1, the federated UKF reduces the attitude error from 0.8 (in the star tracker A) to 0.48 (in the master filter), and the FDI algorithm in the federated filter reduces the attitude error in the master filter from 0.48 to 0.02.

The performance of the proposed algorithm is summarized in Table 2. Each failure in the gyroscope and the star tracker A is considered to verify the fault-tolerant performance of the federated UKF. The errors between true quaternion and the global estimate in the master filter are integrated regardless of the fault isolation. A single UKF is additionally simulated for comparison with the federated UKF. The federated UKF is beneficial in two respects. First, compared with the single UKF, the error sum of the federated UKF is significantly decreased from 145.21 to 12.69 in the gyroscope failure case, and from 89.40 to 40.96 in the star tracker A failure case, respectively. As shown in Figs. 8 and 14, the federated filter accommodates the fault effect in the local sensors even though any FDI logic is not included. Second, the error sum of the federated UKF including fault detection and isolation is remarkably decreased from 12.69 to 1.00 in the gyroscope failure case, and from 40.96 to 1.28 in the star tracker A failure case, respectively. As shown in Figs. 10 and 16, the FDI algorithm enhances the estimation performance by providing robust and accurate global estimate of the satellite attitude. Note that the error sum of the star tracker failure is larger than the error sum of the gyroscope failure because the star tracker provides more accurate measurement than the gyroscope.

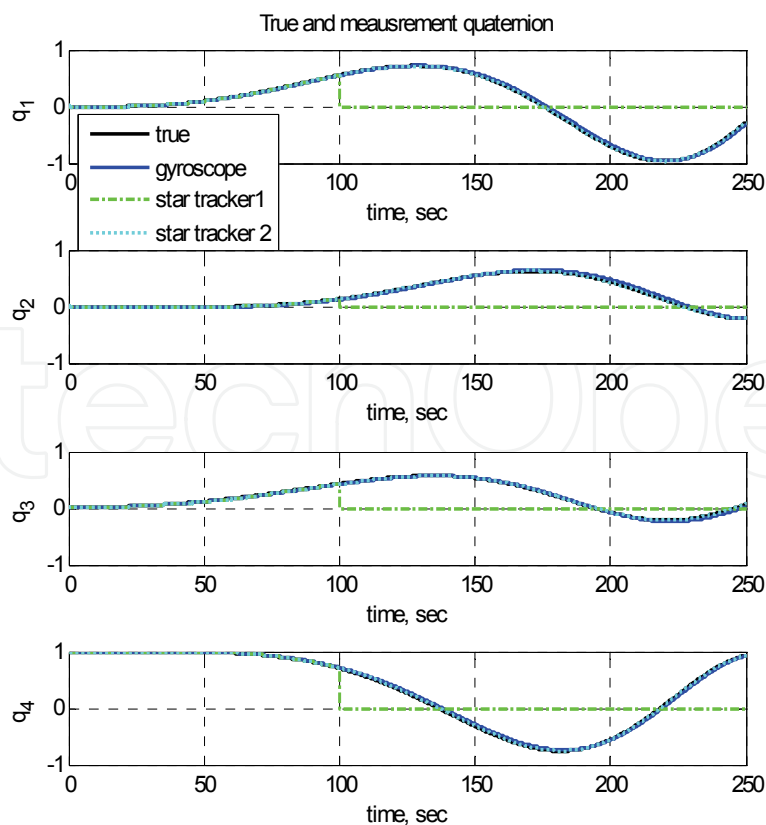


Fig. 12. Quaternion history (star tracker fault)

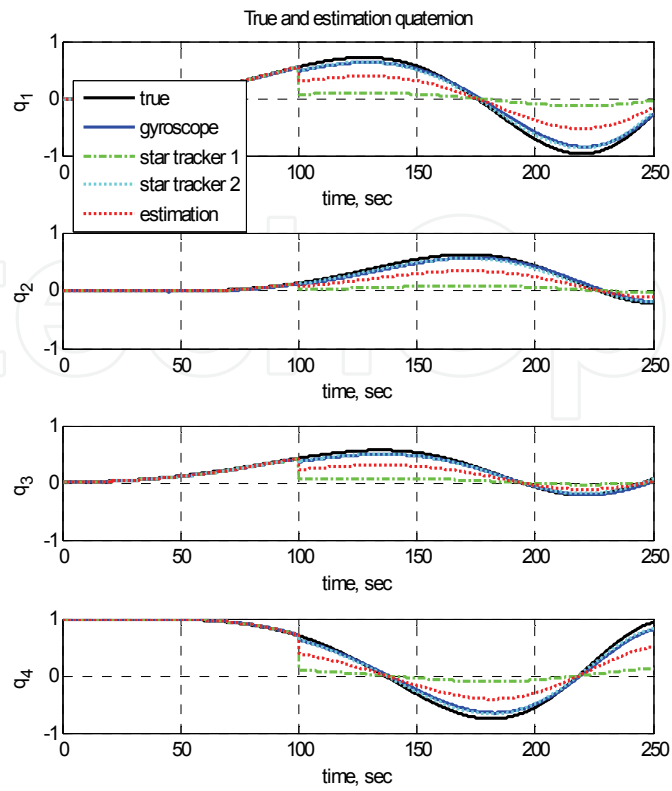


Fig. 13. Local and global estimates without FDI algorithm (star tracker fault)

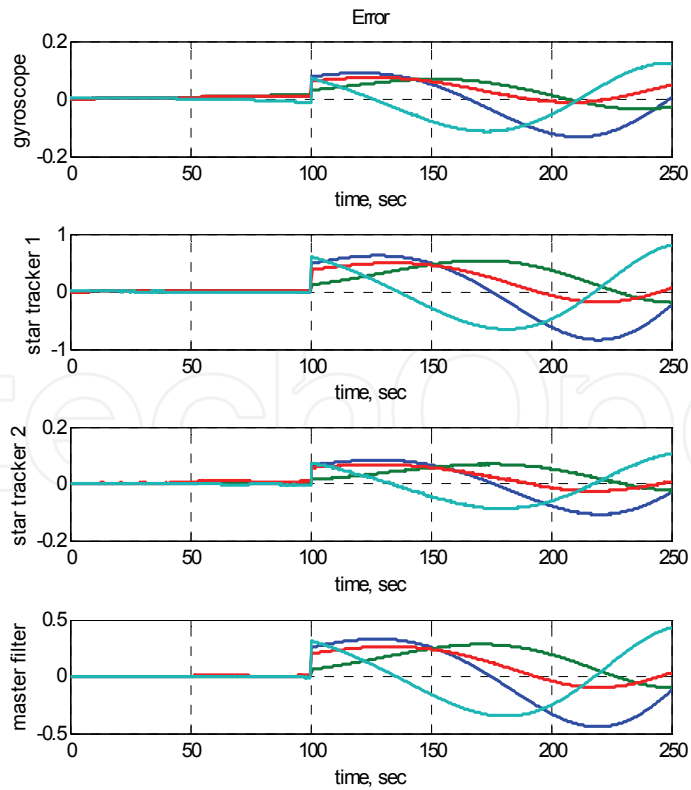


Fig. 14. Error between true quaternion and estimates without FDI algorithm (star tracker fault)

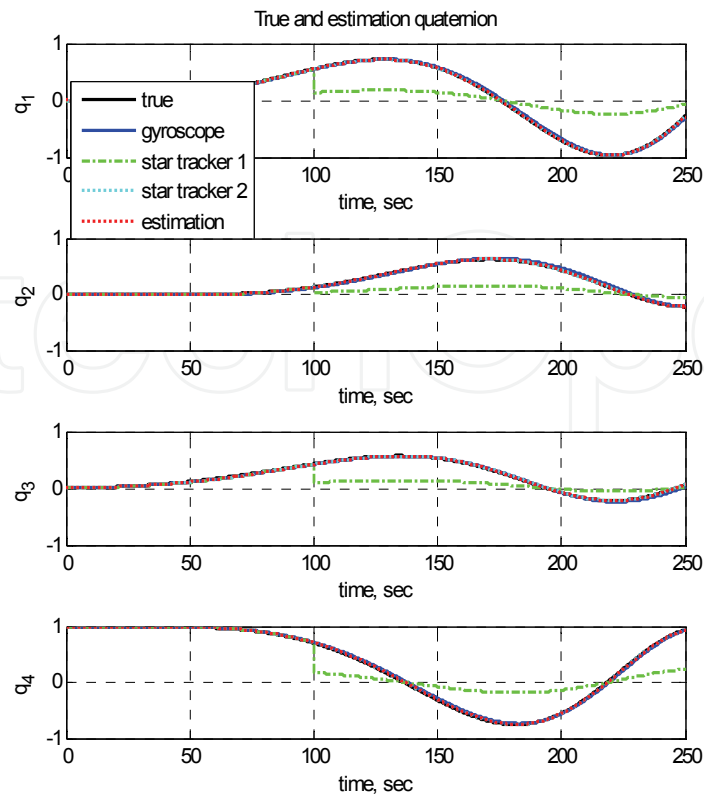


Fig. 15. Local and global estimates with FDI algorithm (star tracker fault)

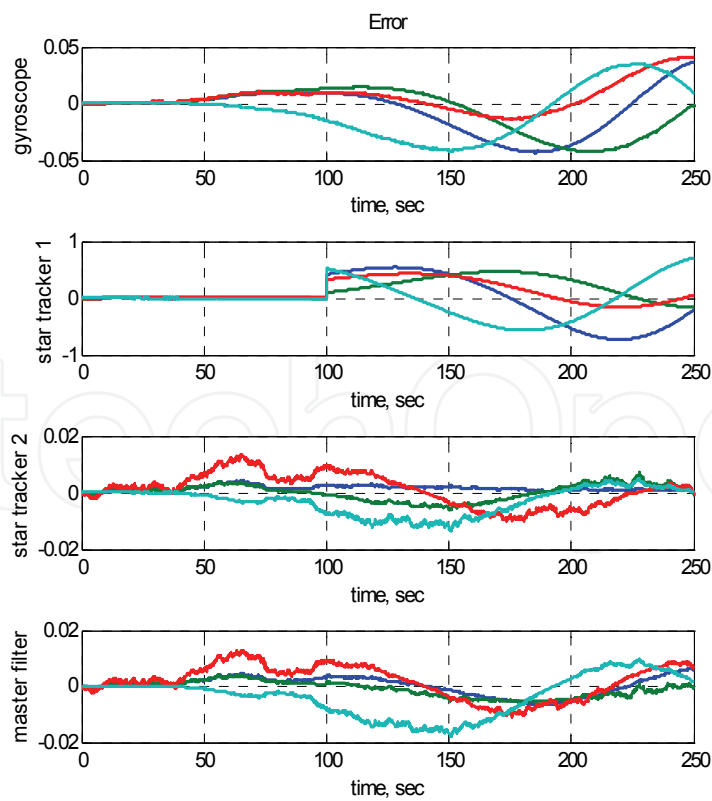


Fig. 16. Error between true quaternion and estimates with FDI algorithm (star tracker fault)

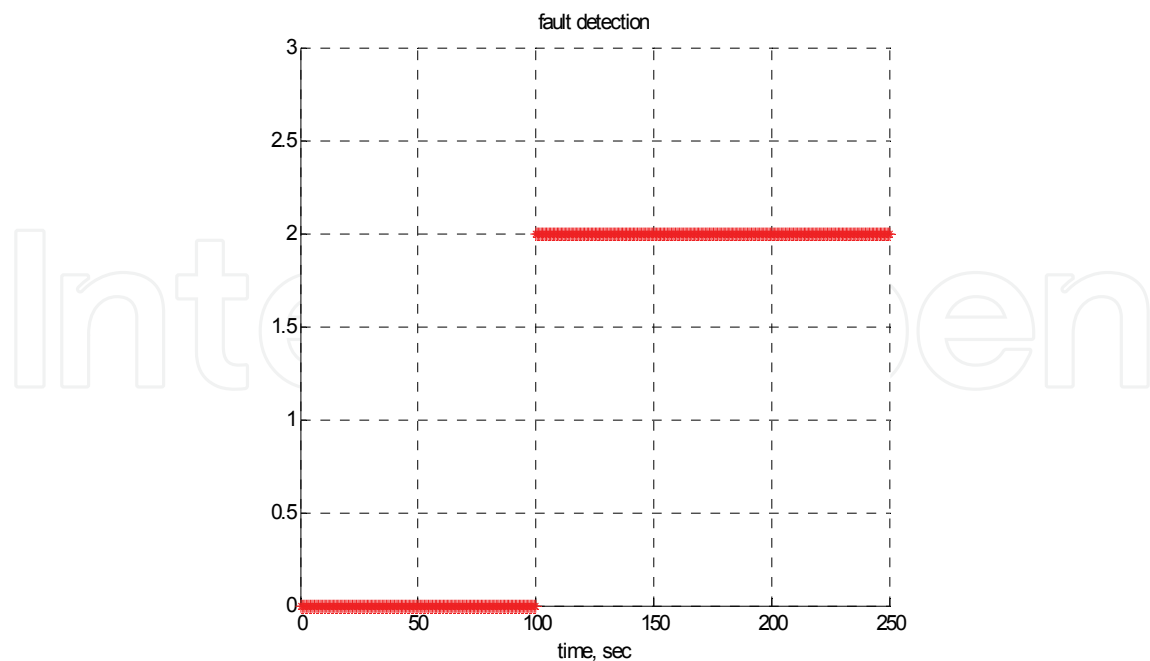


Fig. 17. Fault detection index (star tracker fault)

Sensor Fault Type	Single UKF	Federated UKF	
		Without FDI	With FDI
Gyroscope failure	145.2083	12.6870	1.0022
Star tracker failure	89.4021	40.9636	1.2780

Table 2. Error sum of attitude estimates

## 5. Conclusion

In this study, the federated UKF with the FDI algorithm is proposed for the estimation of the satellite attitude. The UKF gives the accurate estimates for nonlinear systems, and the federated UKF makes the system fault-tolerant and reliable. Since the FDI algorithm can detect and isolate the sensor failure immediately, the global estimate is not affected by the poor local estimate due to the faulty sensor. In this respect, the error of the global estimate using the federated UKF and the FDI algorithm is smaller than that using the federated UKF only. Numerical simulation results show that the proposed algorithm provides efficient and accurate attitude estimation of the satellite despite the fault of the attitude sensors. The proposed algorithm can be applied not only for the satellite systems but also for the ground mobile robots and aerial robot systems.

## 6. References

- Agrawal, B. N. & Palermo, W. J. (2002). Angular Rate Estimation For Gyroless Satellite Attitude Control. *AIAA Guidance, Navigation, and Control Conference*, Monterey, CA, Aug. 2002.

- Bae, J. & Kim, Y. (2010). Attitude Estimation for Satellite Fault Tolerant System using Federated Unscented Kalman Filter. *International Journal of Aeronautical and Space Science*, Vol. 11, No. 2, 2010, pp. 80-86, ISSN: 1229-9626.
- Crassidis, J. L. & Markley, F. L. (2003). Unscented Filtering for Spacecraft Attitude Estimation. *Journal of Guidance, Control, and Dynamics*, Vol. 25, No. 4, 2003, pp. 536-542, ISSN: 0731-5090.
- Edelmayer, A. & Miranda, M. (2007). Federated Filtering for Fault Tolerant Estimation and Sensor Redundancy Management in Coupled Dynamics Distributed Systems. *Mediterranean Conference on Control and Automation*, Athens, Greece, July 2007.
- Hwang, I.; Kim, S.; Kim, Y. & Seah, C.E. (2010). A Survey of Fault Detection, Isolation, and Reconfiguration Methods. *IEEE Transactions on Control Systems Technology*, Vol. 18, No. 3, May 2010, pp.636-653, ISSN: 1063-6536.
- Jayaraman, P.; Fischer, J.; Moorhouse, A. & Lauer, M. (2006). Star Tracker Operational Usage in Different Phases of the Mars Express Mission. *SpaceOps 2006 Conference*, Rome, Italy, June 2006.
- Jiancheng, F. & Ali, J. (2005). Multisensor Data Synthesis using Federated Form of Unscented Kalman Filtering. *IEEE International Conference on Industrial Technology*, Hong Kong, Dec. 2005.
- Jin, Y.; Liu, X. & Hou, C. (2008). Relative Attitude Determination for Fly-Around Based on UKF. *7th World Congress on Intelligent Control and Automation*, Chongqing, China, Jun. 2008.
- Julier, S. J. & Uhlmann, J. K. (2004). Unscented Filtering and Nonlinear Estimation. *Proceedings of the IEEE*, Vol. 92, No. 3, 2004, pp. 401-422, ISSN: 0018-9219.
- Karlgaard, C. D. & Schaub, H. (2008). Adaptive Huber-Based Filtering Using Projection Statistics: Application to Spacecraft Attitude Estimation. *AIAA Guidance, Navigation, and Control Conference*, Honolulu, HI, Aug. 2008.
- Kerr, T. (1987). Decentralized Filtering and Redundancy Management for Multisensor Navigation. *IEEE Transactions on Aerospace and Electronic Systems*, Vol. 20, No. 1, 1987, pp. 83-119, ISSN: 0018-9251.
- Kim, Y. S. & Hong, K. S. (2003). Decentralized Information Filter in Federated Form. *SICE Annual Conference*, Fukui, Japan, Aug. 2003.
- Lee, D. (2008). Unscented Information Filtering for Distributed Estimation and Multiple Sensor Fusion. *AIAA Guidance, Navigation, and Control Conference*, Honolulu, HI, Aug. 2008.
- Mehra, R. & Bayard, D. (1995). Adaptive Kalman Filtering, Failure Detection and Identification for Spacecraft Attitude Estimation. *4th IEEE Conference on Control Application*, Albany, NY, Sep. 1995.
- Nagendra, R. G.; Alex, T. K. & Seetharama, B. M. (2002). Incremental-Angle and Angular Velocity Estimation Using a Star Sensor. *Journal of Guidance, Control, and Dynamics*, Vol. 25, No. 3, 2002, pp. 433-441, ISSN: 0731-5090.
- Schaub, H. & Junkins, J. L. (2003). *Analytical Mechanics of Space Systems*, American Institute of Aeronautics and Astronautics, ISBN: 1-60086-721-9, Reston, VA.
- Simon, D. (2006). *Optimal State Estimation*, Wiley-Interscience, ISBN: 0471708585, Malden, MA.
- Wei, M. & Schwarz, K. P. (1990). Testing a Decentralized Filter for GPS/INS Integration. *Position Location and Navigation Symposium*, Las Vegas, NV, Mar. 1990.
- Xu, Y. (2009). Nonlinear Robust Stochastic Control for Unmanned Aerial Vehicles. *Journal of Guidance, Control, and Dynamics*, Vol. 32, No. 4, 2009, pp. 1308-1319, ISSN: 0731-5090.



## **Advances in Spacecraft Technologies**

Edited by Dr Jason Hall

ISBN 978-953-307-551-8

Hard cover, 596 pages

**Publisher** InTech

**Published online** 14, February, 2011

**Published in print edition** February, 2011

The development and launch of the first artificial satellite Sputnik more than five decades ago propelled both the scientific and engineering communities to new heights as they worked together to develop novel solutions to the challenges of spacecraft system design. This symbiotic relationship has brought significant technological advances that have enabled the design of systems that can withstand the rigors of space while providing valuable space-based services. With its 26 chapters divided into three sections, this book brings together critical contributions from renowned international researchers to provide an outstanding survey of recent advances in spacecraft technologies. The first section includes nine chapters that focus on innovative hardware technologies while the next section is comprised of seven chapters that center on cutting-edge state estimation techniques. The final section contains eleven chapters that present a series of novel control methods for spacecraft orbit and attitude control.

### **How to reference**

In order to correctly reference this scholarly work, feel free to copy and paste the following:

Jonghee Bae, Seungho Yoon and Youdan Kim (2011). Fault-Tolerant Attitude Estimation for Satellite Using Federated Unscented Kalman Filter, *Advances in Spacecraft Technologies*, Dr Jason Hall (Ed.), ISBN: 978-953-307-551-8, InTech, Available from: <http://www.intechopen.com/books/advances-in-spacecraft-technologies/fault-tolerant-attitude-estimation-for-satellite-using-federated-unscented-kalman-filter>

**INTECH**  
open science | open minds

### **InTech Europe**

University Campus STeP Ri  
Slavka Krautzeka 83/A  
51000 Rijeka, Croatia  
Phone: +385 (51) 770 447  
Fax: +385 (51) 686 166  
[www.intechopen.com](http://www.intechopen.com)

### **InTech China**

Unit 405, Office Block, Hotel Equatorial Shanghai  
No.65, Yan An Road (West), Shanghai, 200040, China  
中国上海市延安西路65号上海国际贵都大饭店办公楼405单元  
Phone: +86-21-62489820  
Fax: +86-21-62489821

© 2011 The Author(s). Licensee IntechOpen. This chapter is distributed under the terms of the [Creative Commons Attribution-NonCommercial-ShareAlike-3.0 License](#), which permits use, distribution and reproduction for non-commercial purposes, provided the original is properly cited and derivative works building on this content are distributed under the same license.

IntechOpen

IntechOpen